IOP Publishing Environ. Res. Lett. 16 (2021) 125007 https://doi.org/10.1088/1748-9326/ac3603

ENVIRONMENTAL RESEARCH
LETTERS

CrossMark

OPEN ACCESS

RECEIVED
27 June 2021

REVISED
26 October 2021

ACCEPTED FOR PUBLICATION
3 November 2021

PUBLISHED
25 November 2021

LETTER

High NH_3 deposition in the environs of a commercial fattening pig farm in central south China

Wuying Yi[1,2,3], Jianlin Shen[2,3,*], Guoping Liu[4], Juan Wang[2,3], Lifei Yu[1,*], Yong Li[2,3], Stefan Reis[5,6] and Jinshui Wu[2,3]

[1] Key Laboratory of Plant Resource Conservation and Germplasm Innovation in Mountainous Region (Ministry of Education), Collaborative Innovation Center for Mountain Ecology and Agro-Bioengineering (CICMEAB), College of Life Sciences/Institute of Agro-Bioengineering, Guizhou University, Guiyang 550025, Guizhou Province, People's Republic of China

[2] Key Laboratory of Agro-Ecological Processes in Subtropical Regions, Institute of Subtropical Agriculture, Chinese Academy of Sciences, Changsha 410125, Hunan Province, People's Republic of China

[3] Changsha Research Station for Agricultural and Environment Monitoring, Institute of Subtropical Agriculture, Chinese Academy of Science, Changsha 410125, Hunan Province, People's Republic of China

[4] College of Animal Science, Yangtze University, Jingzhou 424025, Hubei Province, People's Republic of China

[5] UK Centre for Ecology and Hydrology, Bush Eush Estate, Penicuik, Midlothian EH26 0QB, United Kingdom

[6] University of Exeter Medical School, European Centre for Environment and Health, Knowledge Spa, Truro TR1 3HD, United Kingdom

[*] Authors to whom any correspondence should be addressed.

E-mail: jlshen@isa.ac.cn and gdyulifei@163.com

Keywords: NH_3, dry deposition, nitrogen deposition, emission, intensive pig farm

Supplementary material for this article is available online

Abstract

Intensive livestock production has been increasing, and has resulted in the emission of more than seven teragram per year of ammonia (NH_3) in China in recent years. However, little is known about the fate of the emitted NH_3, especially the dry deposition of NH_3 in the environs of intensive animal farms. In this study, the spatial and temporal variations of NH_3 deposition in the environs of an intensive fattening pig farm were investigated in the central south of China. NH_3 concentrations were measured at sites situated 50, 100, 200, 300, and 500 m in the downwind direction from the farm each month from July 2018 to June 2019. The NH_3 deposition was calculated based on a bidirectional NH_3 exchange model. The monthly NH_3 emissions from the pig farm were estimated based on the breeding stock. The annual average NH_3 concentrations ranged from 1200 to 14 μg m^{-3} at the downwind sites within 500 m of the pig farm, exhibiting exponential decay as distance increased. Strong seasonality in NH_3 deposition was observed, with the highest season being in the summer and lowest in the winter, and air temperature was found to be an important factor affecting this seasonal variation. The estimated monthly total dry deposition within 500 m of the pig farm ranged from 92 to 1400 kg NH_3–N mo^{-1}, which accounted for 4.1%–14% of the total monthly NH_3 emissions from the pig farm. The estimated total NH_3 emissions and NH_3 deposition from the pig farm were 63 000 kg NH_3–N yr^{-1} and 5400 kg NH_3–N yr^{-1}, respectively, with the annual average ratio of NH_3 deposition to NH_3 emission being 8.6%. This study found NH_3 deposition around intensive pig farms is high, and determined it as a significant fate of the NH_3 emitted from pig farms.

1. Introduction

NH_3 is a highly reactive and alkaline gas with detrimental human health and ecological impacts (Gourley *et al* 2012, Zhang *et al* 2020). It originates from both natural and anthropogenic sources, with agriculture being its major source (Van Damme *et al* 2018, Guo *et al* 2020, Mueller and Lassaletta 2020). The NH_3 emissions originating from the agricultural sector activities dominantly contribute to total anthropogenic NH_3 emissions, for example, above 80% on a global scale (Mencaroni *et al* 2021), 90% in Europe (Jacobsen *et al* 2019), and 88% in China (Zhang *et al* 2018). Other non-agricultural emission sources include industries (Cui *et al* 2013), urban waste (Elser *et al* 2018, Shao *et al* 2020), transport

(Fenn et al 2018), residential (Bhattarai et al 2020), power plants (Wu et al 2020), and biomass burning (Yu et al 2020). Anthropogenic NH_3 emissions contribute significantly to secondary aerosol formation, and thus contribute to the widespread regional haze and affect human health (Sutton et al 2008, Behera et al 2013, Bao et al 2019, Giannakis et al 2019).

The excess N input via atmospheric NH_3 deposition has noticeably detrimental effects on ecosystems, including soil acidification (Shen et al 2018), N_2O emission enhancement (Xie et al 2018), and eutrophication and acidification of surface and ground water (Scudlark et al 2005, Zhan et al 2017). For example, the atmospheric deposition of NH_3 is a potential acid input, as recently described by Wang et al (2018). Soil acidification has been observed near feedlots owing to high local NH_3 deposition (Shen et al 2018). Xie et al (2018) reported high N_2O emissions from a nitrogen-saturated subtropical forest in China. In addition, NH_3 deposition has become an important source of N content in surface water for the lakes, and may trigger the eutrophication and acidification of surface water (Scudlark et al 2005, Zhai et al 2009, Zhan et al 2017).

Intensive animal farms are known as 'hotspots' for NH_3 emissions (Shen et al 2018). These NH_3 emissions return to the earth's surface via wet or dry deposition. NH_3 may completely dominate the overall load of reactive nitrogen (N_r) from the atmosphere near intense livestock farms (Zapletal and Mikuska 2019). Recent studies have reported NH_3 deposition from poultry facilities (Walker et al 2014, Baker et al 2020) and from typical intensive feedlots (Shen et al 2018, Zapletal and Mikuska 2019, Lassman et al 2020). Within a radius of 150–1000 m from the sources, approximately 3%–16% of NH_3 emissions deposit near the farms (Fowler et al 1998, Hao et al 2006, Walker et al 2008, Shen et al 2018, Zapletal and Mikuska 2019). Pig production is one of the largest sources of NH_3 emissions in China (Xu et al 2017). However, there are few studies on the NH_3 deposition in the environs of the commercial fattening pig farms. Furthermore, only a few studies have specifically investigated the links between NH_3 emissions from typical animal facilities and NH_3 deposition around these sources. The research objectives of this study were (a) to quantify NH_3 dry deposition within 500 m of the edge of an intensive commercial fattening pig farm in the central south of China, and to analyse the seasonal variations of NH_3 deposition; and (b) to gain insight into the relationship between NH_3 emissions and NH_3 deposition around the pig farm. Through this study, we can also know how much the emitted NH_3 or its derivative (e.g. particulate ammonium) will be transported to long distance. By quantifying the NH_3 deposition gradient around the pig farm, we can also further study the impacts of NH_3 deposition on the neighbouring natural ecosystems along a natural gradient.

2. Materials and methods

2.1. Experimental site

The study was conducted at an intensive commercial fattening pig farm in Junchuan town (31°38′53″N, 113°13′48″E) located in Suizhou City, Hubei Province, China (figure 1). The study region is a hilly forested area, approximately 18 km away from the city of Suizhou. The altitude ranged from 90 to 127 m above the mean seal level. The annual precipitation was 940 mm. The average annual temperature was 15.6 °C. Winds were predominantly northerly, while relative humidity ranged between 39% and 99%, during the sampling periods. The dominant soils were Alumi-Ferric Alisols, Haplic Luvisols, and Anthraqui-umbric Gleysols, based on the Food and Agriculture Organization of the United Nations soil classification.

Land use within 500 m of the farm was divided into five categories (figure 1). The total area within 500 m of the farm covered 135 ha, which consisted of 53% forest, 17% arable land, 13% surface water, 9% shrubs, and 8% construction land (7% rural residential, and 1% traffic infrastructure).

The daily pig population in the building ranged from 1330 to 13 400 heads, with an average of 8900 heads. The fattening cycle lasted approximately 110 d. The studied farm had two pig houses set up in the south–north direction. The slurry facility is located next to the pig houses, where pig manure was piled and stored openly (figure 1). Fresh slurry from the pig house was cleared daily and added to the manure pile.

2.2. NH_3 emissions estimation

2.2.1. Pig building

In this study, the method reported by Zhu (2007) was used to estimate NH_3 emissions from a pig farm. The main sources of NH_3 emissions were manure and urine generated by the animals in the barn. The predictive models to estimate daily NH_3 emissions per pig were established by building relationships between the influencing factors (e.g. temperature, ventilation rate, nitrogen content of manure) of NH_3 emissions, and the NH_3 emissions of pig manure or urine per unit mass. These influencing factors were identified mainly based on the understanding of the processes of NH_3 emissions from pig farms. Similar studies for estimating NH_3 emissions from pig farms can be found in Aneja et al (2001), Harper et al (2004), and Ni et al (1999). Because significant differences were observed in the parameter values in the abovementioned studies, we just used the parameters in the study of Zhu (2007), which was conducted in China. The NH_3 emissions for pig manure per unit mass were calculated using equation (1):

$$F_{NH_3} = -20.70 + 0.50T + 5.15V - 0.88D_F + 2.98\,[N_F]\ \left(R^2 = 0.81\right) \quad (1)$$

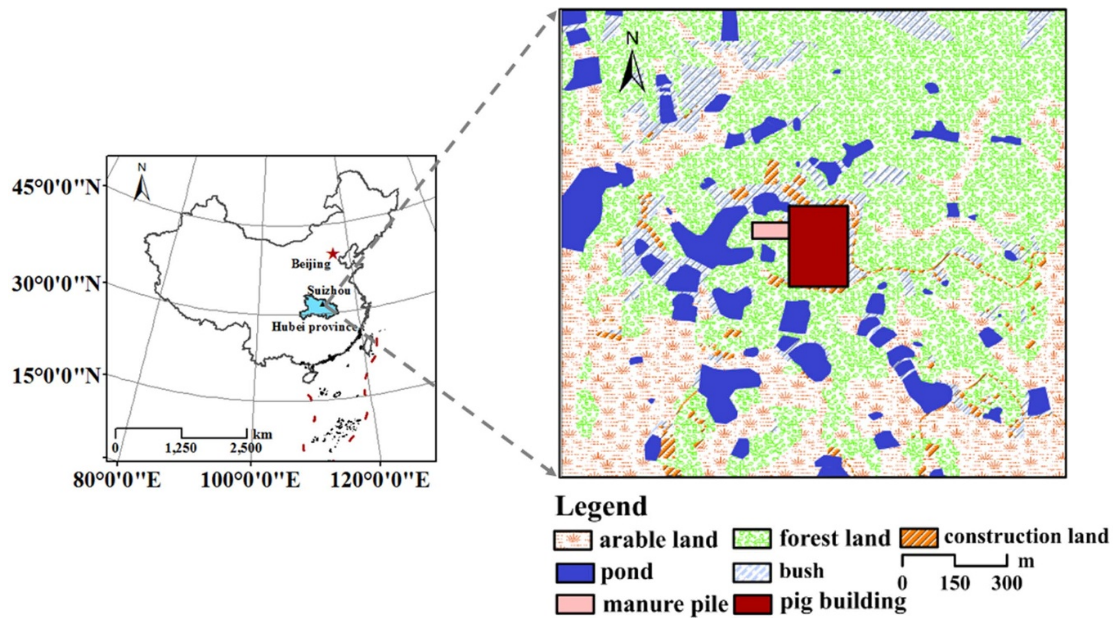

Figure 1. Left: location of the investigated area in Suizhou city, Hubei province, China. Right: the study farm and the land use in the surrounding area of the farm. Image from GoogleEarth©2018, Maxar Technologies. Imagery date: 31 December 2018.

where F_{NH3} is the NH_3 emissions of pig manure per unit mass in kg kg^{-1}, and T is the indoor temperature of the pig house, in °C (23 °C–28 °C). V is the ventilation rate in L min^{-1}, D_F is the depth of pig manure in cm, and $[N_F]$ is the nitrogen content of pig manure in g kg^{-1} (23 g kg^{-1}).

The D_F is calculated using equations (2) and (3):

$$D_F = 100 \times \left(M_{Fpig}/\rho_F\right)/S \quad (2)$$

$$S = 600/P_{barnpig} \quad (3)$$

where M_{Fpig} is the weight of pig manure per head per day in kg head^{-1}, ρ_F is the density of pig manure in kg m^{-3} (1005.9 kg m^{-3}), S is the area per pig in the barn in m^2 head^{-1}, $P_{barnpig}$ is the pig population of the barn (unit: head), 100 is the conversion factor from m to cm, and 600 is the area available for pigs in the barn in m^2.

The fitted equation (4) for calculating the NH_3 emissions of pig urine per unit mass (U_{NH3}) is expressed as follows:

$$U_{NH_3} = 7.14 + 2.39T + 5.14V - 0.74D_U + 0.87[N_U]\ (R^2 = 0.71) \quad (4)$$

where U_{NH3} is the NH_3 emission of pig urine per unit mass in kg kg^{-1}, D_U is the depth of pig urine in cm, and $[N_U]$ is the nitrogen content of pig urine in g l^{-1} (2.85 g l^{-1}).

The D_U is calculated using equation (5):

$$D_U = V_{Upig}/S/1000 \quad (5)$$

where V_{Upig} is the volume of urine per head per day in l head^{-1}, and 1000 is the conversion factor from l to m^3.

The manure and urine production per pig per day were calculated using the model according to the First National Census of Pollution: Manual of Discharge Coefficient of Livestock and Poultry Industry (IEDA and NIES 2009). The total daily manure and urine production were calculated using equations (6)–(10):

$$M_{Fpig} = 1.18 \times \left(W^{0.75}/74^{0.75}\right) \quad (6)$$

$$M_F = M_{Fpig} \times P_{pigbuilding} \quad (7)$$

$$V_{Upig} = 3.18 \times \left(W^{0.75}/74^{0.75}\right) \quad (8)$$

$$V_U = V_{Upig} \times P_{pigbuilding} \quad (9)$$

$$M_U = V_U \times \rho_U/1000 \quad (10)$$

where M_{Fpig} is the weight of pig manure per head per day in kg head^{-1}, W is the mean pig weight in kg, M_F is the total daily manure production in kg, $P_{pigbuilding}$ is the daily pig population in the building (unit: head), V_U is the volume of the total daily urine production in the building in l, V_{Upig} is the volume of urine per head per day in l head^{-1}, M_U is the mass of the total daily pig urine production in the building in kg, ρ_U is the density of pig urine in kg m^{-3} (1000.3 kg m^{-3}), 1.18 is the given pollution coefficient per pig in kg head^{-1}, 74 is the reference weight of pig (74 kg), 3.18 is the given pollution coefficient per pig in l head^{-1}, and 1000 is the conversion factor, from l to m^3.

The daily NH_3 emissions from the pig building (B_{NH3}, kg) were calculated using equation (11):

$$B_{NH3} = M_F \times F_{NH3} + M_U \times U_{NH3}. \quad (11)$$

2.2.2. Manure pile

The cumulative NH_3 emissions of daily manure production from the open-pile storage of pig manure were calculated using equation (12) as follows:

$$M_{NH3j} = \left(\left(\left(M_{Fj}/\rho_F\right)/H\right) \times f_{NH_3}/1000\right) \times (N-j) \quad (12)$$

where M_{NH3j} is the cumulative NH_3–N emissions from manure pile on day j in kg, M_{Fj} is the total daily manure production on day j in kg, H is the height of the manure pile in m (0.5 m), f_{NH3} is the emission factor of pig manure pile in g NH_3–N m^{-2} d^{-1} (3.5 g NH_3–N m^{-2} d^{-1}) (Shan *et al* 2019), N is the number of days in a month in d, j is the jth day of the month in d, and 1000 is the conversion factor, from g to kg.

2.2.3. Total NH_3 emissions

Monthly and annual NH_3 emissions were extrapolated from the daily NH_3 emissions. Monthly and annual NH_3 emissions were calculated using equations (13) and (14) as follows:

$$E_{\text{Tolmonthi}} = \sum_{j}^{N} \left(B_{NH_{3ij}} + M_{NH_{3ij}}\right) \quad (13)$$

$$E_{\text{Tolyear}} = \sum_{i}^{M} E_{\text{Tolmonthi}} \quad (14)$$

where $E_{\text{Tolmonthi}}$ is the NH_3 emissions in the ith month in kg, B_{NH3ij} is the NH_3 emissions from the pig building on the jth day of the ith month in kg, M_{NH3ij} is the cumulative NH_3 emissions from the pig manure pile on the jth day of the ith month in kg; N is the number of days in month i; E_{Tolyear} is the annual NH_3 emissions in kg; and M is the number of months in a year.

2.3. NH_3 concentration monitoring

The NH_3 concentrations were measured using the active denuder for long-term atmospheric (DELTA) sampling system (Tang *et al* 2001, 2009, Sutton *et al* 2001a, 2001b, Zhu *et al* 2021). NH_3 samples were collected each day for five continuous days in the middle or towards the end of each month between July 2018 and June 2019. According to the prevailing direction during the sampling periods, NH_3 air concentrations were measured along one of the eight transects (north, northeast, east, southeast, south, southwest, west, and northwest) downwind of the pig farm. The DELTA systems were placed at five distances from the farm (50, 100, 200, 300, and 500 m), and one system was placed 200 m upwind of the pig farm to measure background NH_3 levels. NH_3 concentrations were measured at 1.5 m above ground level in the open areas. The methods for samples preparing, extraction and analysis were detailed in Tang *et al* (2009). In this study, the quality control method described in Tang *et al* (2009) was referred to assure the quality of the measured NH_3 concentrations.

2.4. NH_3 dry depositions flux calculation

According to Nemitz *et al* (2001) and Shen *et al* (2016), the NH_3 dry deposition around the pig building in this study was estimated using a bi-directional NH_3 exchange model. Based on equations (15)–(17), the total NH_3 dry deposition flux (F_t) can be calculated as follows:

$$x_c = \frac{x_a \times (R_a + R_b)^{-1} + x_s \times \left[(R_a \times R_s)^{-1} + (R_b \times R_s)^{-1} + \left(R_g \times R_s\right)^{-1}\right] + x_g \times \left(R_b \times R_g\right)^{-1}}{(R_a \times R_b)^{-1} + (R_a \times R_s)^{-1} + (R_a \times R_w)^{-1} + \left(R_b \times R_g\right)^{-1} + (R_b \times R_s)^{-1} + (R_b \times R_w)^{-1} + \left(R_g \times R_s\right)^{-1} + \left(R_g \times R_w\right)^{-1}} \quad (15)$$

$$x(z_0) = \frac{x_a - {R_a}^{-1} + x_g \times {R_g}^{-1} + x_c \times {R_b}^{-1}}{{R_a}^{-1} + {R_g}^{-1} + {R_b}^{-1}} \quad (16)$$

$$F_t = \frac{x_a - x(z_0)}{R_a} \quad (17)$$

where x_c is the canopy NH_3 compensation point; and R_a, R_b, R_g, R_s, R_w, x_g, and x_s are the aerodynamic resistance, quasi-laminar boundary layer resistance, in-canopy resistance to the ground, stomatal resistance, circular resistance, ground layer NH_3 compensation point, and stomatal compensation point, respectively. The seven parameters listed above were calculated according to the methods reported by Wesely (1989) for R_g, R_s and R_w, Erisman and Draaijers (1995) for R_a and R_b, and Massad *et al* (2010) for x_g and x_s. x_a is the measured NH_3 concentration. $x(z_0)$ is the NH_3 concentration at the height $d + z_0$, d is the zero-plane displacement height, z_0 is the surface roughness length, and F_t is the total NH_3 dry deposition flux. More information about the bi-directional NH_3 exchange model can also be found in Zhu *et al* (2021).

In theory, NH_3 deposition principally occurs in the downwind areas of pig farms (Shen *et al* 2016). In this study, the background NH_3 concentrations were relatively high (mean: 7.9 μg N m^{-3}, maximum:

17.3 μg N m^{-3}, and minimum: 2.1 μg N m^{-3}), which were near the average NH_3 concentration at rural monitoring sites (8.2 μg N m^{-3}) in 2018 in China (Wen *et al* 2020). The background NH_3 concentration was used to calculate background NH_3 deposition using equation (17). NH_3 deposition in the downwind area caused by NH_3 emissions from the pig farm was then calculated by subtracting the background NH_3 deposition from the total NH_3 deposition in the downwind area (Yi *et al* 2020). The area within 500 m of the pig farm was divided into eight downwind sectors based on a combination of eight major wind directions (shown in figure S1 available online at stacks.iop.org/ERL/16/125007/mmedia). Each downwind site was further divided into five sub-areas: (a) area within 50 m from the pig farm, (b) area between 50 and 100 m from the pig farm, (c) area between 100 and 200 m from the pig farm, (d) area between 200 and 300 m from the pig farm, and (e) area between 300 and 500 m from the pig farm. The monthly NH_3 deposition in the downwind area was calculated by multiplying the frequency of wind direction in a month with the accumulated NH_3 deposition in five sub-areas of the downwind area. The monthly NH_3 deposition flux within 500 m from the pig farm was then calculated using equation (18):

$$T_{Dk} = \sum_{i=1}^{8}\sum_{j=1}^{5} A_{ij} D_j f_i / 1000 \tag{18}$$

where T_{Dk} is the monthly NH_3 deposition (kg N mo^{-1}) in the area located 500 m away from the pig farm, in month k, A_{ij} is the size (ha) of the jth sub-area of the ith downwind area; the summation of A_{ij} is the total downwind area (ha); D_j is the NH_3 deposition rate (kg N ha^{-1} mo^{-1}) in the jth sub-area; f_i is the frequency of the ith wind direction in a year; and 1000 is the unit conversation factor.

By summing the monthly NH_3 deposition, the total annual NH_3 deposition within 500 m of the pig farm (T_D, kg N yr^{-1}) was obtained using equation (19):

$$T_D = \sum_{k=1}^{12} T_{Dk}. \tag{19}$$

3. Results

3.1. Monthly NH_3 emissions from the pig farm

In this study, the emissions from the pig building and manure storage facilities were estimated to be 63 100 kg NH_3–N yr^{-1}. The pig building was the largest source of total NH_3 emissions (>90%) in the farm, as shown in figure 2. The monthly NH_3 emissions of the pig building for the period between July 2018 and June 2019 ranged from 2100 to 10 000 kg, with an average of 5210 kg. The daily NH_3 emissions ranged from 25 kg NH_3–N d^{-1} to 400 kg NH_3–N d^{-1}, with an average of 173 kg NH_3–N d^{-1}. The mean NH_3 emissions rate in the study was calculated to be 17.9 g NH_3–N head^{-1} d^{-1}.

3.2. Monthly mean NH_3 concentrations at downwind sites

The NH_3 concentrations in the study exhibited significant spatial-temporal variations, as shown in figure 3(a). The highest NH_3 concentration at 50 m was 1210 μg N m^{-3}, while the highest concentrations at 100, 200, 300, and 500 m were 1080, 848, 510, and 168 μg N m^{-3}, respectively. During the 12 months sampling period, the mean NH_3 concentrations were 445, 320, 211, 143, and 68 μg N m^{-3} at distances of 50, 100, 200, 300, and 500 m downwind from the pig farm, respectively. From 50 to 500 m downwind, NH_3 concentrations decreased by approximately 85%. The NH_3 concentrations showed a clear seasonal pattern (figure 3(b)). High concentrations of NH_3 occurred mainly in summer, whereas NH_3 concentrations in autumn and spring declined rapidly and reached the minimum level in winter.

3.3. Monthly NH_3 dry depositions in the environs of the pig farm

The monthly NH_3 deposition fluxes also varied strongly in space and in time (table 1), ranging from 0.03 to 8.7 μg N m^2 s^{-1} from July 2018 to June 2019. NH_3 deposition fluxes declined significantly as distance from the farm increased. The highest NH_3 deposition fluxes generally occurred at a distance of 50 m, while the lowest NH_3 deposition fluxes were observed at a distance of 500 m. Table 1 depicts the mean monthly NH_3 deposition fluxes during the sampling periods under the land use types of forest, shrubs, paddy, and inland water. There was a large variation in the mean NH_3 deposition fluxes among the four land use types. The NH_3 deposition fluxes of forest, shrubs, paddy and inland water ranged from 0.08–8.8 μg N m^2 s^{-1}, 0.04–7.8 μg N m^2 s^{-1}, 0.12–7.7 μg N m^2 s^{-1}, and 0.03–3.8 μg N m^2 s^{-1}, respectively. NH_3 deposition flux also exhibited a decreasing trend as distance from the pig farm increased (from 50 to 500 m) along the eight transects (figure 4). The estimated total annual NH_3–N deposition in the areas within 500 m of the pig farm to be 5400 kg N yr^{-1} (table 2) or 40 kg N ha^{-1} yr^{-1} as an area-weighted mean.

3.4. Percentage of NH_3 depositions in the environs of pig farms emitting NH_3

The monthly percentage of NH_3 deposition in the 500 m of pig farm due to the NH_3 emissions from the farm to the total NH_3 emissions from the farm was calculated to indicate the fate of emitted NH_3 in the environs of pig farms. The percentage was in the range

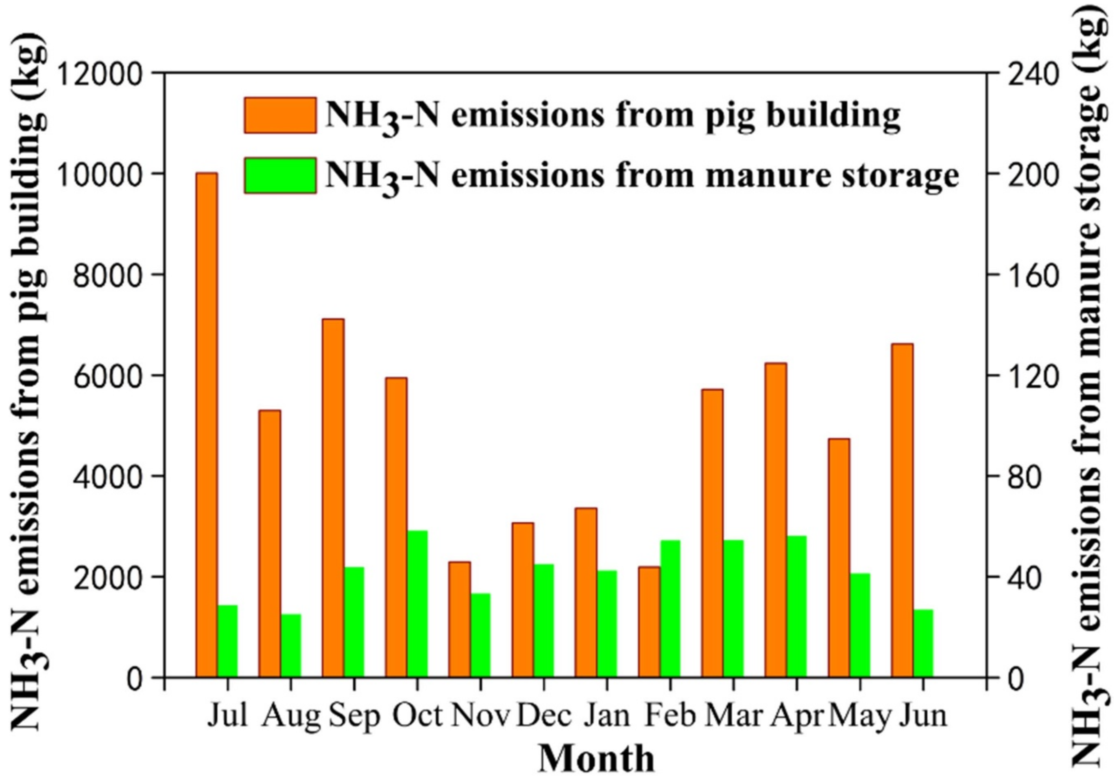

Figure 2. Monthly NH_3 emissions in the pig farm from July 2018 to June 2019.

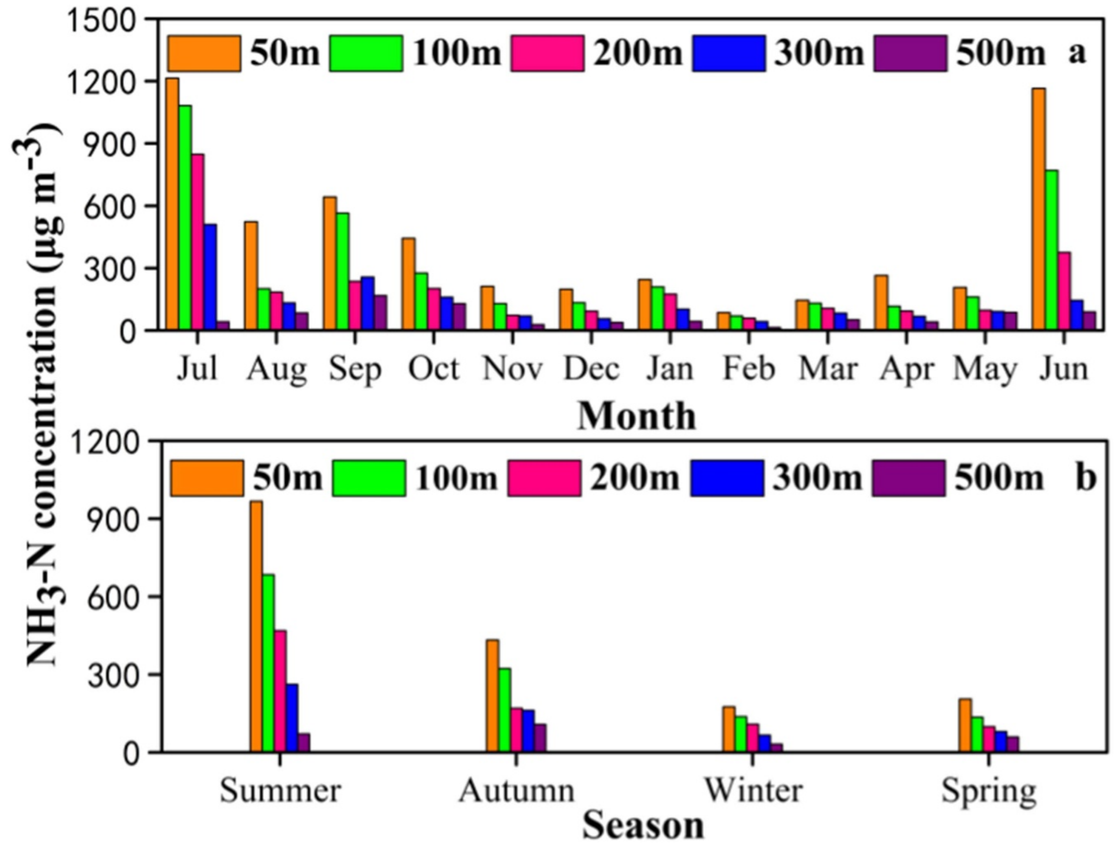

Figure 3. Average monthly and seasonally NH_3 concentrations at downwind sites from July 2018 to June 2019.

Table 1. Mean NH_3 deposition fluxes (μg N m^{-2} s^{-1}) under different land use types during the sampling periods from July 2018 to June 2019.

Site	Distance	Jul	Aug	Sep	Oct	Nov	Dec	Jan	Feb	Mar	Apr	May	Jun
Forest	50 m	8.75	3.64	4.97	2.97	1.19	1.42	1.14	0.51	0.77	1.67	1.12	8.11
	100 m	7.80	1.38	4.37	1.84	0.72	0.95	0.98	0.41	0.69	0.73	0.87	5.36
	200 m	6.10	1.26	1.82	1.35	0.41	0.66	0.81	0.35	0.56	0.58	0.52	2.60
	300 m	3.65	0.90	1.98	1.07	0.39	0.40	0.48	0.25	0.44	0.42	0.48	0.99
	500 m	0.26	0.56	1.29	0.86	0.15	0.27	0.20	0.08	0.27	0.25	0.46	0.61
Shrubs	50 m	7.79	3.45	4.97	2.77	0.61	0.57	0.65	0.25	0.81	1.78	1.03	7.78
	100 m	6.94	1.31	4.37	1.72	0.37	0.38	0.56	0.20	0.72	0.77	0.80	5.14
	200 m	5.43	1.20	1.83	1.26	0.21	0.27	0.46	0.17	0.59	0.62	0.48	2.50
	300 m	3.25	0.86	1.99	1.00	0.20	0.16	0.27	0.12	0.46	0.45	0.45	0.95
	500 m	0.23	0.53	1.30	0.81	0.08	0.11	0.12	0.04	0.28	0.26	0.42	0.59
Paddy	50 m	7.66	2.74	3.41	2.09	1.17	1.04	1.30	0.47	0.83	1.35	0.78	1.37
	100 m	6.82	1.05	3.00	1.30	0.71	0.70	1.11	0.38	0.74	0.59	0.60	0.90
	200 m	5.31	0.96	1.25	0.95	0.40	0.49	0.93	0.32	0.60	0.47	0.36	0.54
	300 m	3.14	0.70	1.36	0.75	0.38	0.29	0.54	0.23	0.47	0.34	0.34	0.29
	500 m	0.12	0.44	0.88	0.60	0.15	0.20	0.23	0.07	0.29	0.20	0.32	0.12
Inland water	50 m	3.76	1.81	2.19	1.15	0.56	0.48	0.62	0.22	0.64	1.13	0.56	0.86
	100 m	3.35	0.69	1.92	0.71	0.34	0.32	0.54	0.18	0.58	0.49	0.43	0.58
	200 m	2.62	0.63	0.80	0.52	0.19	0.22	0.45	0.15	0.47	0.39	0.26	0.37
	300 m	1.56	0.45	0.87	0.41	0.18	0.13	0.26	0.11	0.37	0.28	0.24	0.24
	500 m	0.10	0.27	0.56	0.33	0.07	0.09	0.11	0.03	0.22	0.16	0.23	0.14

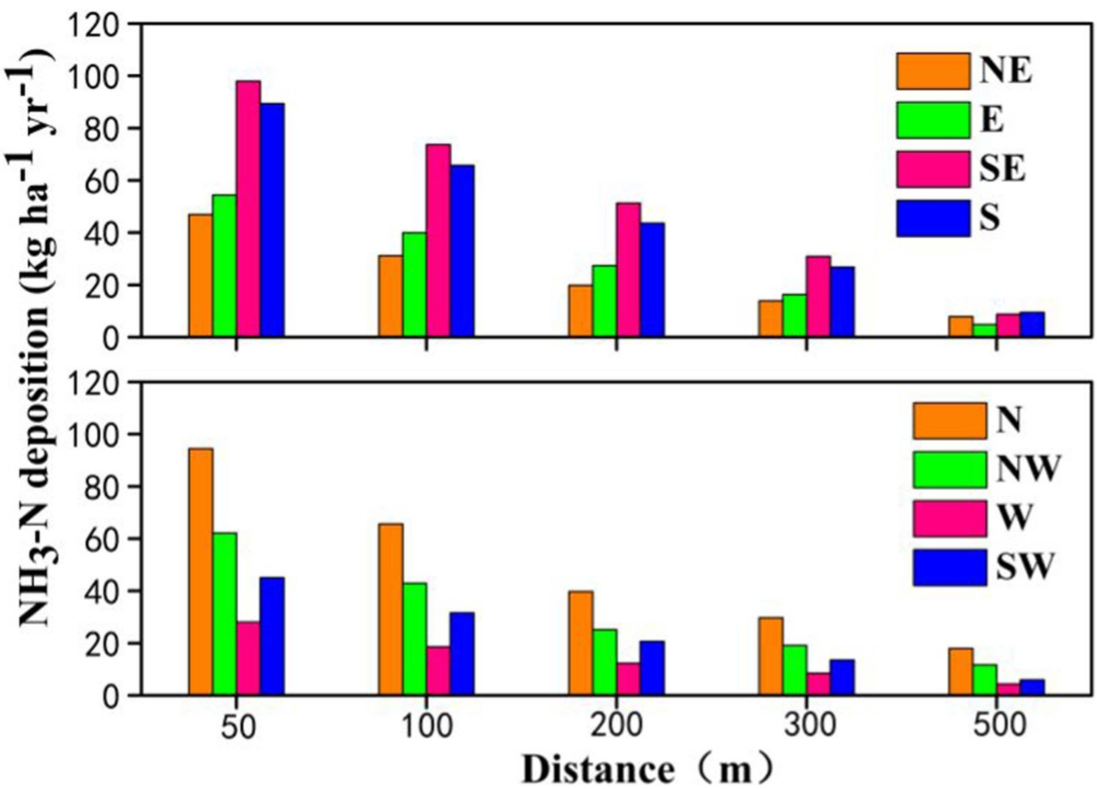

Figure 4. Estimated annual NH_3–N deposition at 50, 100, 200, 300 and 500 m along eight transects (northeast (NE), east (E), southeast (SE), south (S), north (N), northwest (NW), west (W), and southwest (SW)) from July 2018 to June 2019. Note artificial regular spacing on the *x*-axis.

of 4.1%–14%, with an average of 7.6% (shown in figure 5(a)). The percentage was highest in June, and lowest in February. The percentage tendency could be divided into three parts: the percentage sharply decreased from 14% in July to 6% in November; then remained steady in December and January by approximately 6%. Finally, the percentage increased from 4.1% in February to 14% in June. Moreover, the trend of the percentage was consistent with that of the temperature (figure 5(b)).

Table 2. Annual NH_3 depositions in the eight downwind areas within 500 m from the pig farm.

Wind direction	Degree range (°)	Frequency (%)	Downwind area (ha)	NH_3 deposition (kg N yr^{-1})
North	−22.5–22.5	18	28	1090
South	22.5–67.5	8	28	915
East	67.5–112.5	5	27	496
West	112.5–157.5	3	27	265
Northeast	157.5–202.5	7	32	465
Northwest	202.5–247.5	9	32	627
Southeast	247.5–292.5	9	32	1064
Southwest	292.5–337.5	5	32	491
Total		65	238	5413

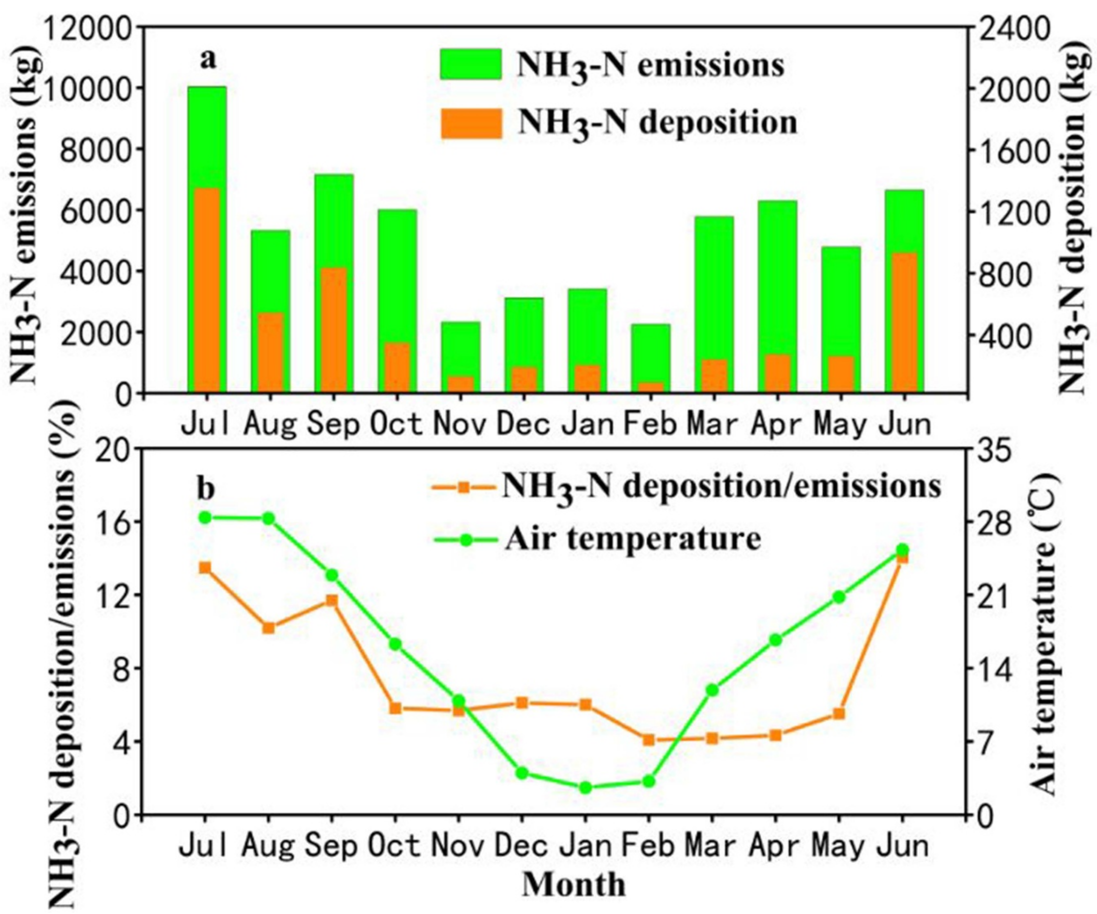

Figure 5. NH_3–N depositions in the total downwind area (135 ha), NH_3–N emissions from the pig farm, the percentage of NH_3 deposition to NH_3 emissions, and air temperature from July 2018 to June 2019.

4. Discussion

4.1. High NH_3 deposition around the pig farm

In this study, NH_3 deposition was high within 500 m of the pig farm. The study's estimates of NH_3 deposition fluxes were higher than those reported in other studies. Walker *et al* (2014) estimated the NH_3 deposition nearby a large poultry facility with 4000 000 laying hens and 750 000 pullets to be 10.1 kg N ha^{-1} yr^{-1} at the refuge boundary, decreasing to 5.4 kg N ha^{-1} yr^{-1} 1500 m. The results of the study conducted by Fowler *et al* (1998) showed that NH_3 deposition close to a large poultry unit of 120 000 broiler chickens declined from 42 kg N ha^{-1} yr^{-1} at 15 m to 5 kg N ha^{-1} yr^{-1} at 270 m, with annual emissions of 4800 kg NH_3–N. Walker *et al* (2008) reported that NH_3 deposition near a swine production facility with a monthly stock of approximately 4900 pigs ranging from 145 kg N ha^{-1} yr^{-1} at 10 m from the source to 16 kg N ha^{-1} yr^{-1} at 500 m, with annual emissions of 34 000 kg NH_3–N. McGinn *et al* (2016) reported a decrease in deposition with distance from the feedlot, with the average stock of 8200 cattle, with deposition decreasing by 50% over 200 m, from 519 to 260 kg N ha^{-1} yr^{-1}. The differences of deposition rates between this and other studies were mainly related to source strength (e.g. animal type, animal population, housing type) and environmental factors (e.g. climate type, terrain, and land use). There were an average stock of 8900 head of pigs in the studied farm, which caused high NH_3 emissions as well as high NH_3 deposition in the environs of the farm. Another possible explanation for the significantly higher NH_3 deposition in the study was the presence of the extensive coniferous forest in the farm environs, which may serve as a barrier to NH_3 horizontal dispersion. Previous studies have also shown that tree belts around farms could be used as an effective way of removing ammonia from the air (Bealey *et al* 2014, 2016). The large NH_3 deposition flux gradient between 50 and 500 m is attributable to the fast dispersion and dilution of the NH_3 plume (Shen *et al* 2016).

In fact, NH_3 will also be wet deposited via scavenging in precipitation or the dry and wet deposition of particulate ammonium, although the component of aerosol ammonium will presumably be negligible compared with gaseous ammonia, since there is insufficient time for NH_3 emissions from the pig farm to convert to ammonium within the 500 m distance from the farm. The annual total precipitation in the study site was approximately 900 mm, thus the lack of estimate of wet deposition of NH_3 might cause the underestimation of the total NH_3 deposition around the pig farm.

Our assessment of the area-weighted mean NH_3 deposition rate (40 kg N ha^{-1} yr^{-1}) indicated higher levels of NH_3 deposition compared with those of typical NH_3 deposition in eastern China known as the NH_3 emission 'hotspot' (deposition 8 kg N ha^{-1} yr^{-1}) (Liu *et al* 2020). The dose effect of NH_3 deposition was based on critical loads (i.e. the deposition levels below which 'significant harmful effects' did not occur (Posch *et al* 2015)). Liu *et al* (2011) suggested that N critical loads for N deposition in subtropical coniferous forests in China were 15–30 kg N ha^{-1} yr^{-1}. In this study, subtropical coniferous forests (Masson pine forest) covered 53% of the study area. The annual average NH_3–N deposition rate within 500 m of the pig farm exceeded the critical load. Excess N may lead to potential risk of soil acidification and cause increased N_2O emissions from the Masson pine forest (Xie *et al* 2018), and result in a decline in forest growth rate (Huang *et al* 2015).

4.2. Seasonal variation of NH_3 deposition

The study showed that meteorological conditions were critical in shaping the seasonality of NH_3 concentrations, which is consistent with the study conducted by Walker *et al* (2014). The seasonal variation in NH_3 deposition was likely caused by environmental factors, such as temperature, precipitation, wind speed, and wind direction (shown in figures S2 and S3). The summer season exhibited the highest NH_3 deposition rate in the downwind area (2800 kg NH_3–N), and NH_3 deposition in autumn, winter, and spring decreased by 53%, 83%, and 72%, respectively, compared with the summer deposition level. Previous results (Jones *et al* 2007) highlighted that NH_3 concentrations directly affect NH_3 deposition. Air temperatures affect the source intensity and soil and vegetation compensation points (Walker *et al* 2014), thus affecting NH_3 concentration in areas downwind of the pig farm. Accordingly, air temperature was a significant variable influencing NH_3 deposition. Previous studies (Cui *et al* 2011, Wen *et al* 2020, Deng *et al* 2021) have shown that precipitation leads to decreased NH_3 deposition. Cook *et al* (2018) suggested that precipitation is not the main driver of N deposition. One possible explanation for this is that the NH_3 depositions in the study area were sufficiently large to obscure the reduction by precipitation, especially in summer. As shown in figure 6, NH_3 deposition and NH_3 emissions were significantly and positively correlated with the monthly mean air temperature. High air temperatures usually favoured a high NH_3 emission rate and caused high NH_3 concentration as well as high NH_3 deposition.

4.3. Low percentage of NH_3 deposition in the neighbourhood to NH_3 emissions from the pig farm

The estimated annual NH_3 deposition (5400 kg N yr^{-1}) in the area within 500 m from the studied pig farm accounted for 8.6% of the annual NH_3 emission (63 100 kg NH_3–N yr^{-1}). The percentage established in this study was compared with that found in other studies, as described in detail below. Fowler *et al* (1998) estimated that 3.8% of the total NH_3 emitted from a poultry farm with 120 000 broilers deposited to the woodland within 270 m from the farm. This study's estimated percentage was substantially lower than that reported by Yi *et al* (2020), which showed that NH_3 deposition in the 100 m neighbourhood of a 0.6 ha paddy field accounted for 80% of the NH_3 emitted from the paddy field. A possible explanation is that a smaller emission intensity of the emission source might lead to a higher percentage in the near-source region. The percentage in this study was lower than that estimated by Hao *et al* (2006) (16%), probably owing to differences in NH_3-emitting source strength (average 8900 heads of pig vs 50 000 heads of cattle). This study's results are slightly lower than those presented by Walker *et al* (2008) at 10%, whose study was conducted within 500 m of a pig farm with natural air flow. The percentage obtained in this study was close to the mean estimate reported by Shen *et al* (2018) and Zapletal and Mikuska (2019), who estimated that NH_3 deposition in the 400–1000 m environs of intensive feedlots accounted for 8% and 12% of the annual NH_3 emissions.

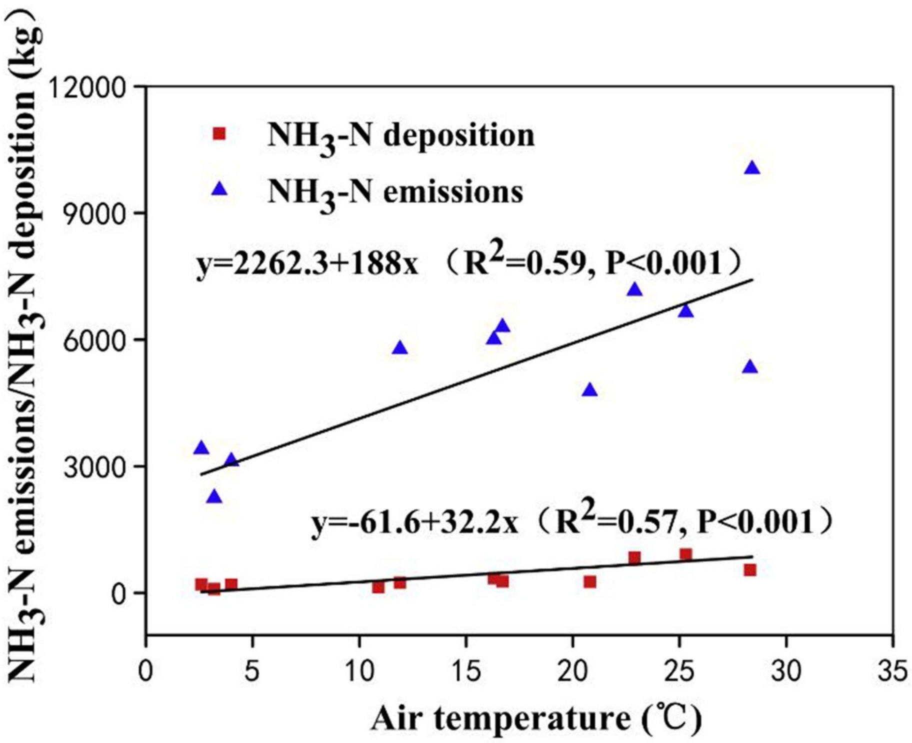

Figure 6. Relationship between air temperature and NH_3 deposition, and NH_3 emissions.

Possible outcomes of additional NH_3 emitted from the farm being retained in the atmosphere without being deposited may be elevation to heights of 100–1500 m within the atmospheric mixing layer (Shen *et al* 2016), or spilling over into non-livestock production regions. The study region was close to cities with two small towns (Junchuan and Anju). The towns and cities produced high concentrations of acidic gas due to heating, transportation, and industry, at a distance of less than 18 km from the farm, which may favour for the formation of secondary aerosols.

4.4. Uncertainty analysis

In this study, NH_3 emissions from the pig farm were estimated using empirical models, thus the values still have some uncertainties. Based on the NH_3 emission factors (11–19 g NH_3–N head^{-1} d^{-1}) for pig from former studies (Balsdon *et al* 2000, Zahn *et al* 2001, Zhang *et al* 2010, Grant *et al* 2016, Ye *et al* 2019), the NH_3 emissions from the pig farm were 38 000–66 000 kg NH_3–N, approximately 60%–104% of our estimation. In the Emission Database for Global Atmospheric Research database, the NH_3 emissions in China as reported by Crippa *et al* (2018), and Janssens-Maenhout *et al* (2015) were estimated based on the NH_3 inventory from Peking University (Huang *et al* 2012), which calculated NH_3 emissions from livestock wastes using the mass flow approach. Based on the Huang's method, as well as the updated Huang's method by Xu *et al* (2017), which reported total daily amount of provincial condition-specific N excretion rate for pigs), the estimated total NH_3 emissions for the studied pig farm was 45 t NH_3–N, which was 71% of the estimated NH_3 emissions of this study. This indicates that our results are still reliable when compared with the former studies.

The uncertainties of the measured NH_3 by DELTA system was approximately 10% (Zhu *et al* 2021). The coefficient of variation for the daily NH_3 concentration and deposition measured at the same location in a month was 6%–19%, which showed relatively stable of NH_3 measurement. Though the bi-directional NH_3 exchange model is theoretically well established, but there are innate challenges in measuring the required parameters. The calculated NH_3 deposition is still subject to uncertainty in the model input parameters (R_a, R_b, R_s, R_w, R_g, x_g and x_s), because parameterization of these variables was mainly using the equations or empirical values based American or European studies. For evaluating the model, we calculated NH_3 dry deposition velocities by dividing the NH_3 deposition fluxes by NH_3 concentrations. The monthly NH_3 deposition velocities were on average 0.5–0.8, 0.3–0.8, 0.1–0.6, and 0.1–0.4 cm s^{-1}, for forest, shrubs, paddy and inland water, respectively. These deposition velocities are comparable with those published mean NH_3 deposition velocities for forest (0.1–3.0 cm s^{-1}), farmland (0.13–0.75 cm s^{-1}) and water (0.5–0.9 cm s^{-1})

(Schrader and Brümmer 2014, Xu *et al* 2015), which indicates that the calculated NH_3 deposition fluxes in this study are in a reasonable range.

5. Conclusions

This study investigated NH_3 concentration measurements at 50, 100, 200, 300, and 500 m downwind of an intensive fattening pig farm with an average stock of 8900 animals in the central south of China from July 2018 to June 2019. The NH_3 deposition exhibited strong seasonality, which was mainly influenced by the temperature. The annual average NH_3 concentrations ranged from 1200 to 14 μg m^{-3} in the downwind direction within 500 m from the pig farm, exhibiting exponential decrease as the distance from the pig farm increased. Monthly NH_3 deposition ranged between 92 and 1400 kg NH_3–N mo^{-1}, which accounted for 4.1%–14% of the total monthly NH_3 emissions from the pig farm. The estimated total NH_3 emissions and deposition from the pig farm were approximately 63 000 kg NH_3–N yr^{-1} and 5400 kg NH_3–N yr^{-1}, respectively, with an annual average percentage of NH_3 deposition to NH_3 emission of 8.6%. The study results suggest that NH_3 deposition around the source of NH_3 is an important result of the emitted NH_3 from pig farms and causes high N input in the pig farm environs. Further measuring and modelling studies are required to explore the effect of the emitted NH_3 from pig farms across areas in far proximity (e.g. more than 500 m).

Data availability statement

The data generated and/or analysed during the current study are not publicly available for legal/ethical reasons but are available from the corresponding author on reasonable request.

Acknowledgments

This study was funded by the National Natural Science Foundation of China (41771336), the National Key Research and Development Program of China (2018YFC0213302), the Chinese Academy of Science and Technology Service Network Initiative Project (KFJ-STS-QYZD-2021-22-002), and the Chinese Academy of Sciences (2017418).

Conflict of interest

The authors declare no competing financial interests.

ORCID iDs

Jianlin Shen https://orcid.org/0000-0002-5853-094X
Stefan Reis https://orcid.org/0000-0003-2428-8320

References

Aneja V P, Bunton B, Walker J T and Malik B P 2001 Measurement and analysis of atmospheric ammonia emissions from anaerobic lagoons *Atmos. Environ.* **35** 1949–58

Baker J, Battye W H, Robarge W, Pal Arya S and Aneja V P 2020 Modeling and measurements of ammonia from poultry operations: their emissions, transport, and deposition in the Chesapeake Bay *Sci. Total. Environ.* **706** 135290

Balsdon S L, Williams J R, Southwood N J, Chadwick D R, Pain B F and Chambers B J 2000 Ammonia fluxes from solid and liquid manure management systems for beef cattle and pigs *Proc. 9th Int. Conf. on the FAO ESCORENA Network on Recycling of Agricultural, Municipal and Industrial Residues in Agriculture* (*Gargano, Italy*, *6–9 September 2000*) ed F Sangiorgi pp 115–20 (available at: http://ramiran.uvlf.sk/doc00/Documents/Session%20II/PA5.pdf)

Bao Z, Chen L, Li K, Han L, Wu X, Gao X, Azzi M and Cen K 2019 Meteorological and chemical impacts on $PM_{2.5}$ during a haze episode in a heavily polluted basin city of eastern China *Environ. Pollut.* **250** 520–9

Bealey W J, Dore A J, Dragosits U, Reis S, Reay D S and Sutton M A 2016 The potential for tree planting strategies to reduce local and regional ecosystem impacts of agricultural ammonia emissions *J. Environ. Monitor.* **165** 106–16

Bealey W J, Loubet B, Braban C F, Famulari D, Theobald M R, Reis S, Reay D S and Sutton M A 2014 Modelling agro-forestry scenarios for ammonia abatement in the landscape *Environ. Res. Lett.* **9** 125001

Behera S N, Sharma M, Aneja V P and Balasubramanian R 2013 Ammonia in the atmosphere: a review on emission sources, atmospheric chemistry and deposition on terrestrial bodies *Environ. Sci. Pollut. Res.* **20** 8092–131

Bhattarai N, Wang S, Xu Q, Dong Z, Chang X, Jiang Y and Zheng H 2020 Sources of gaseous NH_3 in urban Beijing from parallel sampling of NH_3 and NH_4+, their nitrogen isotope measurement and modeling *Sci. Tol. Environ.* **747** 141361

Cook E M, Sponseller R, Grimm N B and Hall S J 2018 Mixed method approach to assess atmospheric nitrogen deposition in arid and semi-arid ecosystems *Environ. Pollut.* **239** 617–30

Crippa M *et al* 2018 Gridded emissions of air pollutants for the period 1970–2012 within EDGAR v4.3.2 *Earth Syst. Sci. Data* **10** 1987–2013

Cui J, Zhou J, Yang H, Peng Y, He Y and Chan A 2011 Atmospheric NO_2 and NH_3 deposition into a typical agro-ecosystem in southeast China *J. Environ. Monitor.* **13** 3216–21

Cui S, Shi Y, Groffman P M, Schlesinger W H and Zhu Y 2013 Centennial-scale analysis of the creation and fate of reactive nitrogen in China (1910–2010) *Proc. Natl Acad. Sci. USA* **110** 2052–7

Deng O, Chen Y, Lan T, Zhang S, Gao X, Zhou W, Ou D, Hu Y and Luo L 2021 Contribution of atmospheric N deposition to riverine N load in a forest-dominated watershed through field monitoring for three years *Chemosphere* **266** 128951

Elser M *et al* 2018 High contributions of vehicular emissions to ammonia in three European cities derived from mobile measurements *Atmos. Environ.* **175** 210–20

Erisman J W and Draaijers G P J 1995 *Atmospheric Deposition in Relation to Acidification and Eutrophication Studies in Environ. Sci.* vol 63 (Amsterdam: Elsevier)

Fenn M E, Bytnerowicz A, Schilling S L, Vallano D M, Zavaleta E S, Weiss S B, Morozumi C, Geiser L H and Hanks K 2018 On-road emissions of ammonia: an underappreciated source of atmospheric nitrogen deposition *Sci. Total. Environ.* **625** 909–19

Fowler D, Pitcairn C E R, Sutton M A, Flechard C, Loubet B, Coyle M and Munro R C 1998 The mass budget of atmospheric ammonia in woodland within 1 km of livestock buildings *Environ. Pollut.* **102** 343–8

Giannakis E, Kushta J, Bruggeman A and Lelieveld J 2019 Costs and benefits of agricultural ammonia emission abatement

options for compliance with European air quality regulations *Environ. Sci. Eur.* **31** 1–13
Gourley C J P, Sharon R A and Powell J M 2012 Nitrogen use efficiency and manure management practices in contrasting dairy production systems *Agric. Ecosyst. Environ.* **147** 73–81
Grant R H, Boehm M T and Heber A J 2016 Ammonia emissions from anaerobic waste lagoons at pork production operations: influence of climate *Agric. For. Meteorol.* **228** 73–84
Guo Y *et al* 2020 Air quality, nitrogen use efficiency and food security in China are improved by cost-effective agricultural nitrogen management *Nat. Food* **1** 648–58
Hao X, Chang C, Janzen H H, Clayton G and Hill B R 2006 Sorption of atmospheric ammonia by soil and perennial grass downwind from two large cattle feedlots *J. Environ. Qual.* **35** 1960–5
Harper L A, Sharpe R R and Simmons J D 2004 Ammonia emissions from swine houses in the southeastern United States *J. Environ. Qual.* **33** 449–57
Huang X, Song Y, Li M, Li J, Huo Q, Cao X, Zhu T, Hu M and Zhang H 2012 A high-resolution ammonia emission inventory in China *Glob. Biogeochem. Cycles* **26** 1–14
Huang Y, Kang R, Mulder J, Zhang T and Duan L 2015 Nitrogen saturation, soil acidification, and ecological effects in a subtropical pine forest on acid soil in southwest China *J. Geophys. Res. Biogeo* **120** 2457–72
IEDA (Institute of Environment and Sustainable Development in Agriculture, Chinese Academy of Agricultural Sciences) and NIES (Nanjing Institute of Environmental Science, Ministry of Environmental Protection of China) 2009 The first national census of pollution: manual of discharge coefficient of livestock and poultry industry Unpublished (in Chinese)
Jacobsen B H, Latacz-Lohmann U, Luesink H, Michels R and Ståhl L 2019 Costs of regulating ammonia emissions from livestock farms near Natura 2000 areas—analyses of case farms from Germany, Netherlands and Denmark *J. Environ. Manage.* **246** 897–908
Janssens-Maenhout G *et al* 2015 HTAP_v2.2: a mosaic of regional and global emission grid maps for 2008 and 2010 to study hemispheric transport of air pollution *Atmos. Chem. Phys.* **15** 11411–32
Jones M R, Leith I D, Fowler D, Raven J A, Sutton M A, Nemitz E, Cape J N, Sheppard L J, Smith R I and Theobald M R 2007 Concentration-dependent NH_3 deposition processes for mixed moorland semi-natural vegetation *Atmos. Environ.* **41** 2049–60
Lassman W Jr., Collett J L, Ham J M, Yalin A P, Shonkwiler K B and Pierce J R 2020 Exploring new methods of estimating deposition using atmospheric concentration measurements: a modeling case study of ammonia downwind of a feedlot *Agr. For. Meteorol.* **290** 107989
Liu L, Zhang X, Xu W, Liu X, Wei J, Wang Z and Yang Y 2020 Global estimates of dry ammonia deposition inferred from space-measurements *Sci. Total. Environ.* **730** 139189
Liu X, Duan L, Mo J, Du E, Shen J, Lu X, Zhang Y, Zhou X, He C and Zhang F 2011 Nitrogen deposition and its ecological impact in China: an overview *Environ. Pollut.* **159** 2251–64
Massad R-S, Nemitz E and Sutton M A 2010 Review and parameterisation of bi-directional ammonia exchange between vegetation and the atmosphere *Atmos. Chem. Phys.* **10** 10359–86
McGinn S M, Janzen H H, Coates T W, Beauchemin K A and Flesch T K 2016 Ammonia emission from a beef cattle feedlot and its local dry deposition and re-emission *J. Environ. Qual.* **45** 1178–85
Mencaroni M, Dal Ferro N, Furlanetto J, Longo M, Lazzaro B, Sartori L, Grant B B, Smith W N and Morari F 2021 Identifying N fertilizer management strategies to reduce ammonia volatilization: towards a site-specific approach *J. Environ. Man.* **277** 111445
Mueller N D and Lassaletta L 2020 Nitrogen challenges in global livestock systems *Nat. Food* **1** 400–1
Nemitz E, Milford C and Sutton M A 2001 A two-layer canopy compensation point model for describing bi-directional biosphere-atmosphere exchange of ammonia *Q. J. R. MeteoR. Soc.* **127** 815–33
Ni J, Vinckier C, Coenegrachts J and Hendriks J 1999 Effect of manure on ammonia emission from a fattening pig house with partly slatted floor *Livest Prod. Sci.* **59** 25–31
Posch M, Duan L, Reinds G J and Zhao Y 2015 Critical loads of nitrogen and sulphur to avert acidification and eutrophication in Europe and China *Landscape Ecol.* **30** 487–99
Schrader F and Bruemmer C 2014 Land use specific ammonia deposition velocities: a review of recent studies (2004–2013) *Water Air Soil Pollut.* **225** 1–12
Scudlark J R, Jennings J A, Roadman M J, Savidge K B and Ullman W J 2005 Atmospheric nitrogen inputs to the Delaware Inland Bays: the role of ammonia *Environ. Pollut.* **135** 433–43
Shan N, Li H, Li J, Ng E L, Ma Y, Wang L and Chen Q 2019 A major pathway for carbon and nitrogen losses—gas emissions during storage of solid pig manure in China *J. Integr. Agr.* **18** 190–200
Shao S, Zhang Y, Chang Y, Cao F, Lin Y, Mozaffar A and Hong Y 2020 Online characterization of a large but overlooked human excreta source of ammonia in China's urban atmosphere *Atmos. Environ.* **230** 117459
Shen J, Chen D, Bai M, Sun J, Coates T, Lam S K and Li Y 2016 Ammonia deposition in the neighbourhood of an intensive cattle feedlot in Victoria, Australia *Sci. Rep.* **6** (available at: www.nature.com/articles/srep32793.pdf)
Shen J, Chen D, Bai M, Sun J, Lam S K, Mosier A, Liu X and Li Y 2018 Spatial variations in soil and plant nitrogen levels caused by ammonia deposition near a cattle feedlot *Atmos. Environ.* **176** 120–7
Sutton M A *et al* 1998 Dispersion, deposition and impacts of atmospheric ammonia: quantifying local budgets and spatial variability *Environ. Pollut.* **102** 349–61
Sutton M A, Erisman J W, Dentener F and Möller D 2008 Ammonia in the environment: from ancient times to the present *Environ. Pollut.* **156** 583–604
Sutton M A, Miners B, Tang Y S, Milford C, Wyers G P, Duyzer J H and Fowler D 2001a Comparison of low cost measurement techniques for long-term monitoring of atmospheric ammonia *J. Environ. Monitor.* **3** 446–53
Sutton M A, Tang Y S, Miners B and Fowler D 2001b A new diffusion denuder system for long-term, regional monitoring of atmospheric ammonia and ammonium *Water Air Soil Pollut. Focus* **1** 145–56
Tang Y S *et al* 2009 European scale application of atmospheric reactive nitrogen measurements in a low-cost approach to infer dry deposition fluxes *Agr. Ecosyst. Environ.* **133** 183–95
Tang Y S, Cape J N and Sutton M A 2001 Development and types of passive samplers for monitoring atmospheric NO_2 and NH_3 concentrations *Sci. World J.* **1** 513–29
Van Damme M, Clarisse L, Whitburn S, Hadji-Lazaro J, Hurtmans D, Clerbaux C and Coheur P-F 2018 Industrial and agricultural ammonia point sources exposed *Nature* **564** 99–103
Walker J T, Robarge W P and Austin R 2014 Modeling of ammonia dry deposition to a pocosin landscape downwind of a large poultry facility *Agr. Ecosyst. Environ.* **185** 161–75
Walker J, Spence P, Kimbrough S and Robarge W 2008 Inferential model estimates of ammonia dry deposition in the vicinity of a swine production facility *Atmos. Environ.* **42** 3407–18
Wang Q, Yu H, Liu J and Li F 2018 Attribution of soil acidification in a large-scale region: artificial intelligence approach application *Soil Sci. Soc. Am. J.* **82** 772–82
Wen Z *et al* 2020 Changes of nitrogen deposition in China from 1980 to 2018 *Environ. Int.* **144** 106022

Wesely M L 1989 Parameterization of surface resistances to gaseous dry deposition in regional-scale numerical models *Atmos. Environ.* **23** 1293–304

Wu C *et al* 2020 Non-agricultural sources dominate the atmospheric NH_3 in Xi'an, a megacity in the semi-arid region of China *Sci. Tol. Environ.* **722** 137756

Xie D, Si G, Zhang T, Mulder J and Duan L 2018 Nitrogen deposition increases N_2O emission from an N-saturated subtropical forest in southwest China *Environ. Pollut.* **243** 1818–24

Xu P, Koloutsou-Vakakis S, Rood M J and Luan S 2017 Projections of NH_3 emissions from manure generated by livestock production in China to 2030 under six mitigation scenarios *Sci. Total. Environ.* **607–8** 78–86

Xu W *et al* 2015 Quantifying atmospheric nitrogen deposition through a nationwide monitoring network across China *Atmos. Chem. Phys.* **15** 12345–60

Ye Z, Guo X, Cheng L, Cheng S, Chen D, Wang W and Liu B 2019 Reducing $PM_{2.5}$ and secondary inorganic aerosols by agricultural ammonia emission mitigation within the Beijing-Tianjin-Hebei region, China *Atmos. Environ.* **219** 116989

Yi Y, Shen J, Yang C, Wang J, Li Y and Wu J 2020 Dry deposition of ammonia around paddy fields in the subtropical hilly area in southern China *Atmos. Ocean. Sci. Lett.* **13** 216–23

Yu X, Shen L, Hou X, Yuan L, Pan Y, An J and Yan S 2020 High-resolution anthropogenic ammonia emission inventory for the Yangtze River Delta, China *Chemosphere* **251** 126342

Zahn J A, Tung A E, Roberts B A and Hatfield J L 2001 Abatement of ammonia and hydrogen sulfide emissions from a swine lagoon using a polymer biocover *J. Air Waste Manage. Assoc.* **51** 562–73

Zapletal M and Mikuska P 2019 Ammonia emissions and dry deposition in the vicinity of dairy farms *Atmosfera* **32** 337–50

Zhai S, Yang L and Hu W 2009 Observations of atmospheric nitrogen and phosphorus deposition during the period of algal bloom formation in Northern Lake Taihu, China *Environ. Manage* **44** 542–51

Zhan X *et al* 2017 Evidence for the importance of atmospheric nitrogen deposition to eutrophic Lake Dianchi, China *Environ. Sci. Technol.* **51** 6699–708

Zhang L *et al* 2018 Agricultural ammonia emissions in China: reconciling bottom-up and top-down estimates *Atmos. Chem. Phys.* **18** 339–55

Zhang X, Gu B, van Grinsven H, Lam S K, Liang X, Bai M and Chen D 2020 Societal benefits of halving agricultural ammonia emissions in China far exceed the abatement costs *Nat. Commun.* **11** 4357

Zhang Y, Dore A J, Ma L, Liu X, Ma W, Cape J N and Zhang F 2010 Agricultural ammonia emissions inventory and spatial distribution in the North China Plain *Environ. Pollut.* **158** 490–501

Zhu H 2007 Study on ammonia emission and model of growing-finishing pigs *PhD Thesis* Chinese Academy of Agricultural Sciences (in Chinese) (available at: https://kreader.cnki.net/Kreader/CatalogViewPage.aspx?dbCode=CDMD&filename=2007156408.nh&tablename=CDFD9908&compose=&first=1&uid=WEEvREcwSlJHSldSdmVqM1BLVW9SZEtIbnd6Z1UvQUxMV3dlVzdMajlPTT0=$9A4hF_YAuvQ5obgVAqNKPCYcEjKensW4IQMovwHtwkF4VYPoHbKxJw!!)

Zhu X, Shen J, Li Y, Liu X, Xu W, Zhou F, Wang J, Stefan R and Wu J 2021 Nitrogen emission and deposition budget in an agricultural catchment in subtropical central China *Environ. Pollut.* **289** 117870